RESEARCH PAPER
https://doi.org/10.1071/WF25255

International Journal of WILDLAND FIRE
International Association of Wildland Fire

Machine learning prediction of fine woody fuel consumption in surface fires burning in eucalypt forest fuels

Yuying Chen[A,B], Andrew L. Sullivan[C], Zilong Wang[B], Liubov Volkova[D], Christopher J. Weston[D], Shaorun Lin[B], Yunzhu Qin[B], Xinyan Huang[B,*] and Nic C. Surawski[A,*]

For full list of author affiliations and declarations see end of paper

***Correspondence to:**
Nic C. Surawski
Centre for Green Technology, University of Technology Sydney, Gadigal Country, PO Box 123, Ultimo, NSW 2007, Australia
Email: Nicholas.Surawski@uts.edu.au

Xinyan Huang
State Key Laboratory of Climate Resilience for Coastal Cities, The Hong Kong Polytechnic University, Kowloon, Hong Kong
Email: xy.huang@polyu.edu.hk

Received: 27 October 2025
Accepted: 6 January 2026
Published: 13 February 2026

Cite this: Chen Y *et al.* (2026) Machine learning prediction of fine woody fuel consumption in surface fires burning in eucalypt forest fuels. *International Journal of Wildland Fire* **35**, WF25255. doi:10.1071/WF25255

© 2026 The Author(s) (or their employer(s)). Published by CSIRO Publishing on behalf of IAWF.
This is an open access article distributed under the Creative Commons Attribution-NonCommercial-NoDerivatives 4.0 International License (CC BY-NC-ND)

OPEN ACCESS

ABSTRACT

Background. Accurate prediction of the woody debris consumed in wildfires is important for both wildland management and carbon accounting. **Aims.** We investigate the combustion factor (defined as the mean diameter reduction rate of the assumed cylindrical woody debris after fire) for fine woody debris (FWD) with pre-burn diameters ranging from 6 to 50 mm in free-spreading surface fires. **Methods.** Experiments were conducted in the CSIRO Pyrotron combustion wind tunnel facility (Canberra, Australia). A database of FWD consumption was constructed from experimental observations featuring 17 predictor variables. Machine learning models were applied to predict the FWD combustion factor. **Key results.** Pearson correlation coefficient analysis indicated that the FWD combustion factor exhibited highly significant negative correlations with smouldering duration, pre-burn diameter and tunnel axial position of FWD. **Conclusions.** We conclude that our combustion wind tunnel experimental approach captures the underpinning fire behaviour physics of FWD consumption well. A binary classification model using a support vector classifier demonstrated the best results for predicting FWD consumption, with an overall classification accuracy of 74%. A ridge regression model achieved a mean absolute error of approximately 9% for modelling FWD consumption. **Implications.** Our results illuminate possible options for controlling woody fuel consumption during managed fires in landscapes.

Keywords: artificial intelligence, binary classification, combustion factor, CSIRO Pyrotron combustion wind tunnel, eucalypt, fine woody debris, fire behaviour, fuel consumption, machine learning, FWD, wildfire, wildland fire.

Introduction

Woody debris (WD) or downed woody material refers to coarse dead fuel elements with a diameter >6 mm that dominate total fuel loads in tropical, temperate and boreal forests (Hollis *et al.* 2011*b*; Van Leeuwen *et al.* 2014; Volkova and Weston 2015). Woody debris plays an important role in forest ecosystems by supporting key ecological processes such as nutrient cycling and soil stabilisation, and represents vital habitat for species, while also contributing to biological diversity (Harmon *et al.* 1986; Hollis *et al.* 2011*a*). Additionally, WD serves as a significant carbon sink, typically capable of storing 5–10% of a forest's total carbon budget (Manies *et al.* 2005), although in some cases, this value can reach 50% (Davis *et al.* 2003). In eucalypt forests (the dominant forest type in Australia), WD constitutes the majority of the ground fuel load and forms the major proportion of fuel consumed by forest fires, which contributes to greenhouse gas and particulate emissions (Volkova *et al.* 2022).

WD plays a significant role in forest fires by influencing fire behaviour (Sullivan *et al.* 2012), emission production (Ottmar 2014) and post-fire ecological processes (Reinhardt *et al.* 2001; Reinhardt 2003). WD typically undergoes three phases of combustion in wildfires: (I) drying and preheating, (II) ignition and flaming combustion, and (III) smouldering and glowing combustion (Sullivan 2017; Hollis *et al.* 2018, 2010). WD ignition typically commences during passage of the flame front but can take some time to

Downloaded from http://connectsci.au/wf/article-pdf/doi/10.1071/WF25255/1856354/wf25255.pdf by The Hong Kong Polytechnic University user on 13 February 2026

become sustained. The delay in sustained ignition depends on both the woody fuel properties and the fire intensity (Hollis *et al.* 2011*b*). Once ignited, WD begins to thermally decompose, producing combustible volatiles and char in thermo-kinetic competition (Sullivan and Ball 2012), both of which can oxidise in the presence of sufficient oxygen – volatiles forming flaming combustion and char forming glowing or smouldering combustion. Volatiles formation and combustion are fast compared with char formation and smouldering combustion, leading to the perception that smouldering occurs after flaming is completed, but this is not necessarily the case. Owing to the relative inefficiency of gas-phase oxygen access to the solid-phase smouldering and the amount of material typically involved, smouldering of WD can persist for a long period of time, sometimes even months after the initiating fire, posing challenges for fire suppression and increasing the risk of re-ignition of other fuels (Kauffman and Martin 1989; Knapp *et al.* 2005; Hyde *et al.* 2011).

The consumption of WD is defined as the amount (i.e. mass or volume) of the woody fuel that is combusted during a fire (Ottmar 2014). Understanding the pre- and post-fire quantities of WD in wildlands is crucial for quantifying fuel heterogeneity (Hyde *et al.* 2011), modelling fire spread (Sullivan *et al.* 2018), and estimating carbon and other gaseous and solid-phase emissions (Ottmar 2014; Prichard *et al.* 2017). Existing literature has shown that the modelled estimates of pollutant emissions are more sensitive to fuel consumption than to the selection of emissions factors (Ottmar *et al.* 2008; Ottmar 2014).

The consumption of WD is affected by multiple factors, such as the physico-chemical properties of fuels, the amount, spacing and orientation of the fuels, and the behaviour and intensity of the initiating fire, which are largely determined by environmental conditions such as air temperature, humidity and wind speed (Hollis *et al.* 2011*a*), as well as the fire spread mode of combustion of the initiating fire, i.e. heading, flanking or backing spread (Surawski *et al.* 2015). Among these factors, woody fuel moisture content is often considered one of the most critical variables influencing fuel consumption (Byram 1959; Albini and Reinhardt 1997; Prichard *et al.* 2017). However, establishing a clear relationship between woody fuel moisture and woody fuel consumption remains challenging owing to the large moisture variability within individual WD pieces and the fact that woody fuel moisture is often correlated with the degree of woody decay (Hollis *et al.* 2011*b*). Wind affects WD consumption by altering the airflow, oxygen availability and fire spread (Finney and McAllister 2011). Some studies show that no significant difference in WD consumption exists between heading and backing fires (Hough 1968). Pre-fire fuel load is another vital parameter (Brown 1985; Hollis *et al.* 2010), with smaller woody fuels (<7.5 cm in diameter) showing significantly higher consumption when pre-fire loads exceed 22.4 t ha^{-1} (Brown 1985). Additionally, a strong positive relationship between WD consumption and fireline intensity has been widely reported across different forest sites (Burrows 2001; Tolhurst *et al.* 2006; Youngblood *et al.* 2008; De Groot *et al.* 2009; Hollis *et al.* 2011*a*). Thus, accurately predicting WD consumption remains a complex challenge.

Various models have been developed to estimate woody fuel consumption and have been incorporated into several software applications, including the empirical CONSUME model (Prichard *et al.* 2007), the process-based Burnout model and hybrid models like BURNUP (Albini and Reinhardt 1997; Reinhardt *et al.* 1997). These models are widely used in the United States and parts of Canada. CONSUME Version 3.0 includes an activity fuel model and a natural fuel model (Ottmar *et al.* 2006). It requires input variables such as fine fuel load, woody fuel load, woody fuel moisture and duff fuel moisture content. For the activity fuel model, additional factors, including burned area, fire duration, slope and mid-flame wind speed are also required. Albini's early Burnout model is a process-based model that simulates fundamental biological and physical processes governing fuel consumption (Albini 1976). BURNUP is an improved and calibrated Burnout model, which predicts the reduction of fuel diameter over time until the fire self-extinguishes or all fuel is consumed, and applies some constants such as heat capacity, thermal conductivity, ignition temperature and char temperature (Albini and Reinhardt 1995).

In Australia, the National Carbon Accounting System applies a Tier 2 country-specific methodology that adopts an assumed woody fuel combustion factor of 50% for wildfires across a broad range of burning conditions (Volkova *et al.* 2019), which could achieve a mean absolute error (MAE) of 11.2% in Australian southern eucalypt forest fires (Hollis *et al.* 2010). The Woody Fuel Consumption Project (WFCP) initiated in 2007 aimed to better understand and model woody fuel consumption in eucalypt forests in southern Australia (Hollis *et al.* 2010). As part of this project, a generalised linear model (GLM) model was developed that is capable of predicting woody fuel consumption for prescribed fires, with an MAE of 12.2% (Hollis *et al.* 2011*a*), that uses fireline intensity as a predictor variable. In addition, the Forest Fire Danger Index, which incorporates the effect of air temperature, relative humidity, wind speed and a drought factor, was identified as the best predictor of woody fuel consumption by a GLM, achieving an R^2 of 0.58 and an MAE of 10% (Hollis *et al.* 2011*b*).

Machine learning is a data-driven approach that enables computers to identify complex patterns and relationships within data. In recent years, machine learning has been widely applied in wildfire science and management for studies that investigate fuel characterisation (Riley *et al.* 2014; López-Serrano *et al.* 2016), fire susceptibility (Duane *et al.* 2015; Hong *et al.* 2018), fire risk assessment (Jafari Goldarag *et al.* 2016) and fire behaviour prediction (Kozik *et al.* 2013; Chetehouna *et al.* 2015). For example, Pierce *et al.* (2012)

Downloaded from http://connectsci.au/wf/article-pdf/doi/10.1071/WF25255/1856354/wf25255.pdf by The Hong Kong Polytechnic University user on 13 February 2026

used a random forest (RF) algorithm to classify the canopy fuel variables used for fire behaviour analysis in Lassen Volcanic National Park, California, using canopy cover, height, base height and bulk density. Different models, such as artificial neural networks (ANN), linear regression (LR), RF and support vector machines (SVM), have been applied for mapping fire susceptibility (Bassett *et al.* 2015; Jain *et al.* 2020; Tang *et al.* 2022). Also, various machine learning models have been developed to predict fire behaviour, including the rate of spread, flame height and flame angle (Chetehouna *et al.* 2015; Hodges and Lattimer 2019). However, the application of machine learning techniques to predict woody fuel consumption in wildland fire science remains unexplored.

This paper aims to develop a predictive model for fine woody debris (FWD) consumption with pre-burn diameters ranging between 6 and 50 mm using machine learning techniques. Predictions of FWD consumption are based on 17 predictor variables that capture the influence of environmental conditions, fuel properties, FWD orientation, FWD configuration and fire behaviour variables. Experiments were previously conducted in the CSIRO Pyrotron combustion wind tunnel at the CSIRO National Bushfire Behaviour Research Laboratory, Canberra, Australia, to obtain empirical estimates of FWD consumption as well as the predictor variables. Once our results database was assembled, various models were trained, evaluated and compared for predicting the FWD combustion factor.

Methodology

Combustion wind tunnel experiments

Laboratory-scale experiments were conducted with the CSIRO Pyrotron, a large combustion wind tunnel facility designed for wildfire research and housed in the CSIRO National Bushfire Behaviour Research Laboratory. This apparatus has been used to undertake fire behaviour (Mulvaney *et al.* 2016; Gould and Sullivan 2021), emissions (Surawski *et al.* 2015; Guérette *et al.* 2025), pyrogenic carbon production (Surawski *et al.* 2020) and suppression studies (Plucinski *et al.* 2017).

The experimental design and set-up were described in detail by Sullivan *et al.* (2018) and were chosen specifically to simulate typical prescribed burning scenarios in dry eucalypt forests in central Victoria, Australia. In summary, the airflow velocity in the tunnel was set at 1.0 m s^{-1}; the fuel bed consisted of dry eucalypt forest litter (leaves, twigs and bark <6 mm diameter) and FWD (6–50 mm diameter) collected from a forest in Victoria (37°28′57.2″S 144°13′24.1″E). As shown in Fig. 1*a*, the working section of the wind tunnel was 4.8 m long and 2.0 m wide and could contain a fuel bed 4.5 m long and 1.5 m wide. For this set of experiments, the fuel bed for heading fires (fire that spreads in the same direction as the wind) was 4.0 m long (Fig. 1*c*), whereas for backing fires (fire that spreads in the direction opposite to the wind), it was 2.0 m long (Fig. 1*d*). As shown in

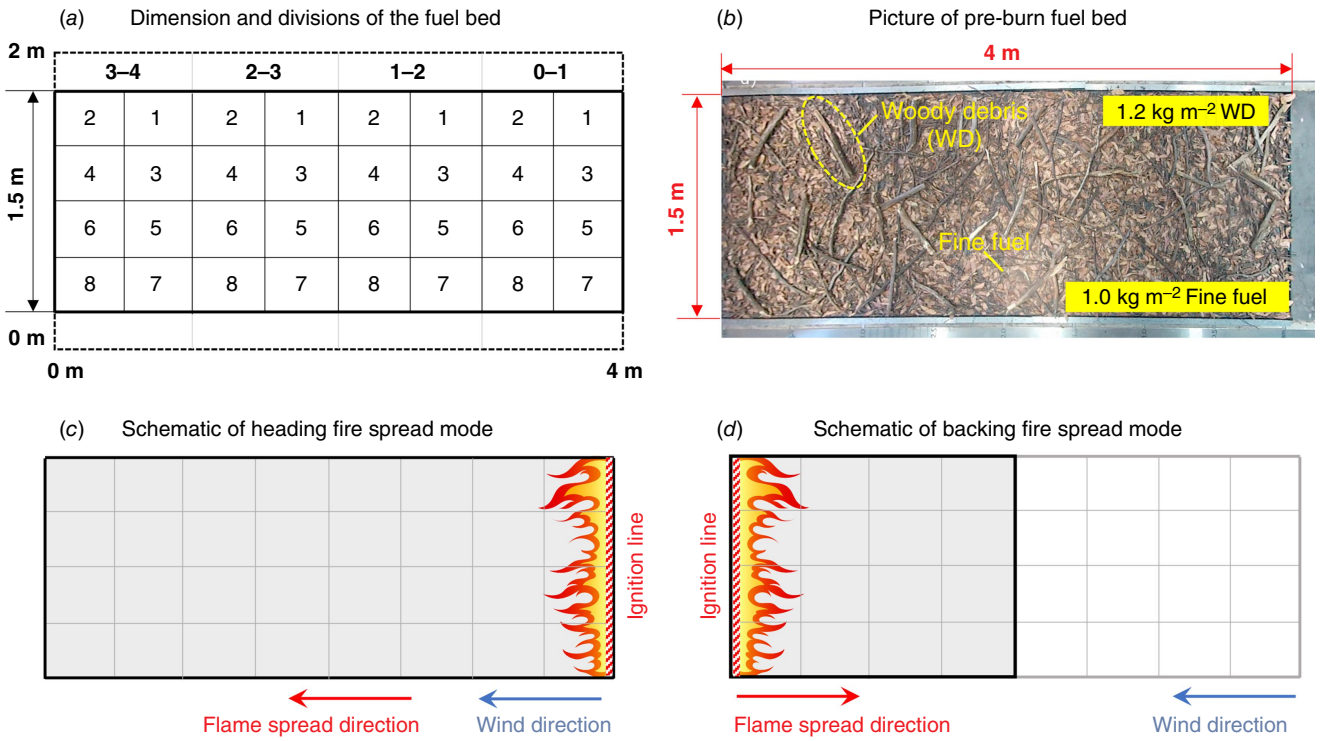

Fig. 1. (*a*) Diagram of the dimensions and division of the fuel bed; (*b*) picture of the fuel bed before fire (under a FWD load of 1.2 kg m^{-2}); and schematic of (*c*) heading, and (*d*) backing fire spread modes, where the black rectangles indicate the area of the fuel bed.

Downloaded from http://connectsci.au/wf/article-pdf/doi/10.1071/WF25255/1856354/wf25255.pdf by The Hong Kong Polytechnic University user on 13 February 2026

Fig. 1*a*, the floor of the working section was manually divided into four horizontal sections that were each 1.0 m in length. Each section was further subdivided into eight equally sized cells 0.5 × 0.375 m to randomly set the position of the FWD pieces using a random number generator. For example, the circled piece of FWD in Fig. 1*b* is positioned in section 3–4 and spans cells 1 and 3.

All fires were ignited using a line ignition method, where a channel spanning the entire width of the fuel bed, as illustrated in Fig. 1*c*, *d*, was filled with 99% ethanol and ignited with a gas lighter to commence each experiment. An array of K-type thermocouples was placed on the Pyrotron floor at 0.5 m intervals along the bed, with 11 thermocouples distributed across the width of the working section to capture the arrival of the flame front. A ceiling-mounted camera in the working section was used to record fire behaviour phenomena for each piece of FWD, such as the location and ignition delay, as well as the durations of flaming and smouldering combustion.

Fig. 1*b* provides an example of the pre-burn fuel bed. Fuels were conditioned under prevailing ambient temperature and humidity conditions in a shed. As a result, the moisture content of the fine fuels ranged from 10.2 to 12.7%, while that of the FWD was approximately 11.5%, commensurate with those of prescribed burning (Sullivan *et al.* 2018).

The surface litter fuel was evenly distributed across the floor of the working section to form the fine fuel bed. The total load of FWD for each experiment (0.2, 0.6, or 1.2 kg m^{-2}) was divided equally between the two size classes, with the smaller 6–25 mm pieces evenly distributed across the fuel bed, and the larger 25–50 mm pieces placed randomly in the fuel bed. The orientation of FWD was randomised using four angles relative to the airflow: parallel (PAR), perpendicular (PER), left 45° (L45) and right 45° (R45). The diameter of each FWD piece before the fire and FWD pieces that were not completely consumed post-fire were measured manually with Vernier callipers at three positions along the length of each fuel element and recorded. The same fine fuel load (i.e. 1.0 kg m^{-2}) was used in all experiments. Further details on fuel collection, preparation and measurements are available in Sullivan *et al.* (2018).

Data collection and database establishment

A total of 18 variables were measured from the experiments to form a database characterising the fire burning dynamics and fire severity for machine learning modelling. Specifically, there are three environmental and operational parameters: ambient temperature (T_a), relative humidity (RH) and fire spread mode (including heading and backing fires). Six parameters were obtained from analysis of experimental videos and laboratory records to describe the properties of the fuel bed and the spacing and configuration of each FWD piece before the fires. These were the FWD fuel load (FL), tunnel axial position and cell position where the FWD was placed, FWD orientation and pre-burn diameter (D_{pre}) of each FWD piece. The FWD combustion factor was defined as the mean diameter reduction of the assumed cylindrical woody debris after fire. Additionally, nine parameters were calculated to characterise the fire behaviour near specific FWD pieces:

(1) Interval rate of spread (ROS_{in}, m s^{-1}) was calculated for each interval between two thermocouple arrays as the ratio of the 0.5-m distance and the time taken for the flame front to spread between adjacent arrays (Gould *et al.* 2017).

(2) Cumulative rate of spread (ROS_{cu}, m s^{-1}) was calculated as the cumulative distance from the ignition line to each 0.5-m thermocouple array divided by the time from ignition to the fire front arriving at each interval (Gould *et al.* 2017).

(3) Interval fireline intensity (FLI_{in}, kW m^{-1}) was calculated as (Byram 1959):

$$FLI_{in} = H \times w \times ROS_{in}, \quad (1)$$

where H is the lower heat of combustion (kJ kg^{-1}), which is typically 18 × 10^3 kJ kg^{-1} for eucalyptus litter and FWD (Sullivan *et al.* 2018), w is the mass of fuel consumed in the active flaming front per unit area (kg m^{-2}) and ROS_{in} is the interval rate of spread (m s^{-1}).

(4) Cumulative fireline intensity (FLI_{cu}, kW m^{-1}) was calculated as:

$$FLI_{cu} = H \times w \times ROS_{cu}, \quad (2)$$

where ROS_{cu} is the cumulative rate of spread (m s^{-1}).

(5) Ignition delay (t_{ig}, s) is the time required for a FWD piece to be ignited after flame arrival. It was calculated as the time when the fuel element commenced flaming combustion minus the time when the flame base arrived at the fuel element.

(6) Residence time (t_{re}, s) described the duration of flaming combustion at a fixed location on the fuel bed, which was determined as the time a FWD was immersed in the flame (Nelson 2003). The ratio of flame depth to interval rate of spread was used to calculate t_{re}.

(7) Duration of flaming combustion (t_{fl}, s) was calculated as the time that flaming combustion ended minus the flame attachment time (i.e. the time when the fuel element commenced flaming combustion).

(8) Duration of smouldering duration (t_{sm}, s) was calculated as the time when visible smoke disappeared minus the burnout time (i.e. the time when flaming combustion ceased).

(9) Charring intensity (CI, °C s) was calculated by integrating the thermocouple data $T(t)$ with the trapezoidal method from when the temperature rose above 200°C (t_0) to when it dropped below 200°C (t_f) (Pyle *et al.* 2015), that is,

$$CI = \int_{t_0}^{t_f} T(t)\,dt. \quad (3)$$

In total, the database included 138 unique observations and for each observation, it included 18 variables. The established

Downloaded from http://connectsci.au/wf/article-pdf/doi/10.1071/WF25255/1856354/wf25255.pdf by The Hong Kong Polytechnic University user on 13 February 2026

experimental dataset is shown in Supplementary material Table S1.

Framework for machine learning modelling

The 'Scikit-Learn' open-source library in Python (Bisong 2019) was used to code the machine learning models in this work. Fig. 2 shows the workflow chart of the machine learning process, which contains three main steps: (1) data pre-processing, (2) classification, and (3) regression modelling. Firstly, the database was pre-processed by normalisation and feature selection to eliminate the scale differences and influence of irrelevant variables. Then, the data were labelled as fully consumed or partially consumed, thus preparing them for the classification step. The labelled data were split into two sets: 70% for the training set and 30% for the test set.

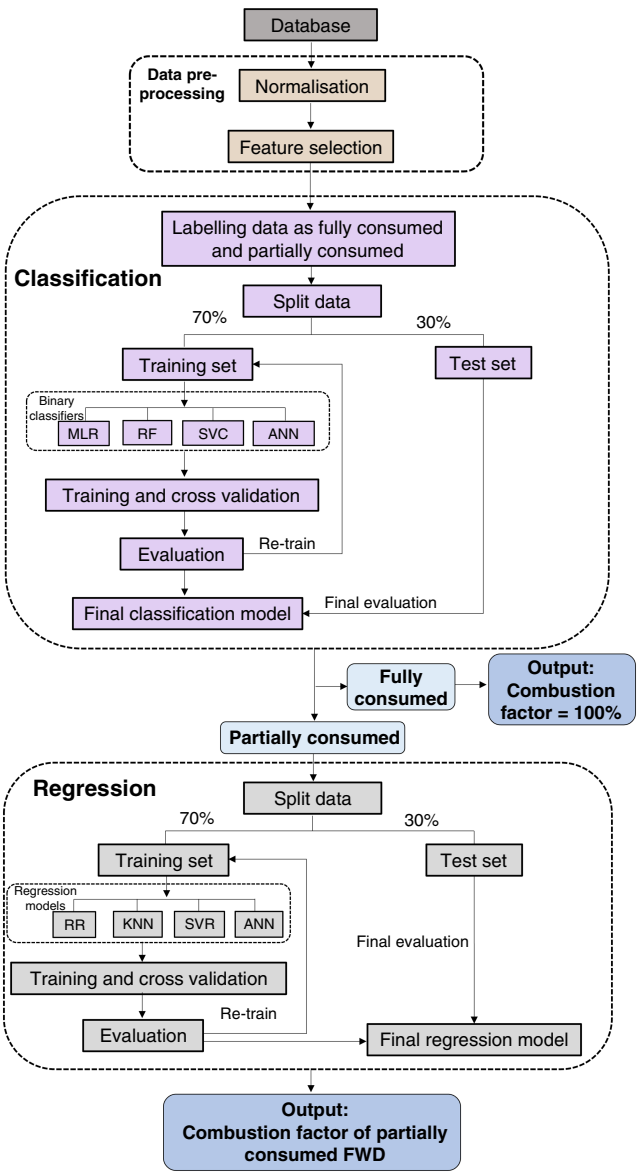

Fig. 2. Workflow of the machine learning prediction procedure.

A classification model was trained with multiple binary classifiers, including LR, RF, support vector classification (SVC) and ANN (discussed in detail in the next section). The best-performing classification model and hyper-parameters were determined by a trial-and-error method within the training set using five-fold cross-validation. In five-fold cross-validation, the dataset was split into five equal parts and the model was trained on four parts and tested on the remaining one, with this process repeated five times using a different test set each time. The cross-validation technique is commonly used to prevent overfitting of the training data (Chen *et al.* 2023). The final classification model predicts whether a FWD piece is fully consumed (i.e. combustion factor is 100%) or partially consumed ($0 \leq$ combustion factor $< 100\%$).

For the data classified as fully consumed, the FWD combustion factor is output as 100%. For the data classified as partially consumed, they moved to a second regression step for the prediction of the combustion factor. For these data, another round of data splitting was performed to create new training and test sets. Given the limited level of experimental replication relative to the number of recorded variables, four regression models were selected to support such datasets. These were ridge regression (RR), *K*-nearest neighbours (KNN), support vector regression (SVR) and ANN. For each model, the best hyper-parameters were determined by a trial-and-error method within the training set using five-fold cross-validation. After that, the trained regression model was used to predict the combustion factor of the partially consumed FWD pieces.

The following section introduces the machine learning (ML) models employed in this work.

Machine learning models

Multiple logistic regression

Multiple logistic regression (MLR) is commonly used in binary classification problems, which is derived from the GLM (LaValley 2008). It uses a logistic function called a sigmoid function (i.e. S-shaped curve) to calculate the probability of occurrence from predictor variables. The following equation represents multiple logistic regression:

$$f(x_i) = \frac{1}{1 + e^{-z}} = \frac{e^{\left(b_0 + \sum_{j=1}^{k} b_j x_{i,j}\right)}}{1 + e^{\left(b_0 + \sum_{j=1}^{k} b_j x_{i,j}\right)}}, \quad (4)$$

where: $f(x_i)$ is the ith predicted output (estimated probability); $x_{i,j}$ represents input data for the ith value of independent variable j, where $i \in \{1, \ldots, n\}$ and $j \in \{1, \ldots, k\}$; b_0 is the bias or intercept term; b_j is a set of coefficients that measures the contribution of each independent variable x_j, n is the number of FWD pieces for which the combustion factor was measured. If the estimated probability is greater

Downloaded from http://connectsci.au/wf/article-pdf/doi/10.1071/WF25255/1856354/wf25255.pdf by The Hong Kong Polytechnic University user on 13 February 2026

than 0.5 (or other user-defined threshold value), the subject is classified into the success group; otherwise, it is classified into the failure group (LaValley 2008).

Random forest

Random forest (RF) is an ensemble learning method that constructs a series of decision trees using bootstrap samples of the original dataset (Breiman 2001). In the RF model, each tree is built from a randomly selected subset of predictors that optimise a splitting criterion at each node. For classification tasks, the final prediction is determined by the consensus of the trees, whereas for regression tasks, it is based on averaging the predictions of individual trees. The model estimates prediction error by using out-of-bag samples, where each tree predicts data not included in its bootstrap sample, providing an internally unbiased estimate of model performance (Liaw and Wiener 2002). The RF model is quite user-friendly because it requires only two parameters that the user needs to define: the number of trees in the forest and the number of predictor variables in the random subset of trees at each node (Breiman 2001).

K-Nearest neighbour

K-Nearest neighbour (KNN) is a supervised machine learning algorithm that can be used for both classification and regression tasks. As KNN performs well with small datasets, it is selected to predict the combustion factor for FWD that is not fully consumed, based on a dataset containing only 67 entries. In regression tasks, KNN predicts the value of a target by averaging the outputs of the k closest data points in the feature space, where proximity is typically measured using a distance metric. The most commonly used distance metrics in KNN include Euclidean distance, Manhattan distance, Minkowski distance and Mahalanobis distance (Altman 1992). KNN is sensitive to the choice of k and the distance metric.

Support vector machine

Support vector machine (SVM) is a supervised learning algorithm that is widely used for both classification and regression tasks, referred to as SVC and SVR, respectively. SVM operates by identifying an optimal hyperplane that separates data points in a high-dimensional space. In SVC, this hyperplane maximises the margin between different classes, whereas in SVR, the goal is to minimise prediction error within a defined tolerance. The model relies on a subset of training samples known as support vectors, which define the position and orientation of the hyperplane; any change in these points can alter the decision boundary or regression function. SVM can effectively handle nonlinear relationships by projecting input features into higher-dimensional spaces using kernel functions, such as a linear kernel function, a sigmoid kernel function, a radial basis function (RBF) and polynomial kernels (Corinna and Vladimir 1995; James *et al.* 2013).

A linear kernel function is given by:

$$K(x_i,\ x_j) = \sum_{k=1}^{p} x_{i,k} \times x_{j,k}, \tag{5}$$

where $x_{i,k}$ and $x_{j,k}$ are separate observations for independent variable k.

A sigmoid kernel function is given by:

$$K(x_i,\ x_j) = \tanh(\alpha \times \sum_{k=1}^{p} x_{i,k} \times x_{j,k} + \beta), \tag{6}$$

where α and β are the slope and offset parameters of the tanh function.

A radial basis kernel function (RBF) is given by:

$$K(x_i,\ x_j) = \exp(-\gamma \sum_{k=1}^{p} (x_{i,k} - x_{j,k})^2), \tag{7}$$

where γ is a positive parameter and can be parameterised as $\gamma = 1/2\sigma^2$ (σ^2 is the bandwidth of the RBF).

A polynomial kernel function is given by:

$$K(x_i,\ x_j) = (\sum_{k=1}^{p} x_{i,k} \times x_{j,k} + r)^d, \tag{8}$$

where r is a constant term and d is the degree of the polynomial.

Artificial neural network

An ANN is a deep-sequence data processing network, which can learn from prior events and establish a pattern to generate the desired result. In this work, the back propagation neural network is used, which is a widely applied ML model in wildfire research (Vasilakos *et al.* 2009; Zhang *et al.* 2021). The backpropagation neural network is a multi-layer feedforward neural network in which model parameters (weights and biases) are iteratively updated using the backpropagation algorithm to minimise prediction error. Typically, the ANN network has an input layer, an output layer and one or multiple hidden layers with an interconnected perceptron.

For each perceptron shown in the ANN network, the output of the jth neuron (O_j) is calculated as:

$$O_j = h(\sum_{i=1}^{N} W_{ji} X_i + B_j), \tag{9}$$

where X_i is the input from the preceding layer neuron, W_{ji} is the weight from input neuron i to output neuron j, B_j is the bias, and h is the transfer (activation) function. Many types of activation functions are available in the 'Scikit-Learn' library (Kartal and Özveren 2022), such as *sigmoid* (or *logistic*), reLU and tanh. In this work, the employed activation functions include reLU and *logistic*, which are stated as follows for the independent variable z:

$$\mathrm{reLU}(z) = \max(0, z), \tag{10}$$

$$\sigma(z) = \frac{1}{1 + e^{-z}}. \tag{11}$$

Downloaded from http://connectsci.au/wf/article-pdf/doi/10.1071/WF25255/1856354/wf25255.pdf by The Hong Kong Polytechnic University user on 13 February 2026

Classification performance evaluation methods

There are many techniques to evaluate the performance of classification models including the confusion matrix, accuracy, precision, sensitivity, specificity, *F*1 score, ROC (receiver operating characteristic) curve and recall (Kartal and Özveren 2022). In the present work, the classification model involves a two-class prediction problem (i.e. binary classification), in which the results are labelled either as 'completely consumed' or 'partially consumed'. Here, the completely consumed result is defined as positive (P) and the partially consumed result is defined as negative (N). Correct predictions include so-called true positives (TP) and true negatives (TN), and incorrect predictions include false positives (FP) and false negatives (FN).

The accuracy measures how often an ML model correctly predicts the outcome:

$$\text{Accuracy} = \frac{\text{TP} + \text{TN}}{\text{TP} + \text{TN} + \text{FP} + \text{FN}}. \quad (12)$$

The precision measures how often an ML model correctly predicts the positive class:

$$\text{Precision} = \frac{\text{TP}}{\text{TP} + \text{FP}}. \quad (13)$$

The recall (also called sensitivity or true positive rate, TPR) measures how often an ML model correctly identifies positive instances from all the actual positive samples in the dataset.

$$\text{TPR} = \frac{\text{TP}}{\text{TP} + \text{FN}}. \quad (14)$$

The FPR (false positive rate) measures the proportion of negative cases that a model incorrectly predicts as positive:

$$\text{FPR} = \frac{\text{FP}}{\text{FP} + \text{TN}}. \quad (15)$$

*F*1 score gives a combined idea about the precision and recall metrics, which is defined as:

$$F1 = 2 \times \frac{\text{Precision} \times \text{TPR}}{\text{Precision} + \text{TPR}}. \quad (16)$$

An ROC curve is a graph of TPR versus FPR, which depicts the relative trade-offs between the false positive and true positive rates at varying threshold values. The performance quality of the models can be calculated by the area under the ROC curve (AUC). The higher the AUC value, the higher the accuracy of the model is.

Regression performance evaluation methods

The performance of the developed regression models is measured by the difference between the predicted and observed values. In this work, three common criteria were used to evaluate the model: MAE in Eqn 17, MSE (mean squared error) in Eqn 18 (Bennett *et al.* 2013), RMSE (square root of the MSE), and R^2 (coefficient of determination) in Eqn 19 (Montgomery and Runger 2010). A larger R^2 and smaller MAE and RMSE indicate better model performance. These fitting criteria are defined as:

$$\text{MAE} = \frac{1}{N} \sum_{i=1}^{N} \left| Y_{\text{observed},i} - Y_{\text{predicted},i} \right|, \quad (17)$$

$$\text{MSE} = \frac{1}{N} \sum_{i=1}^{N} (Y_{\text{observed},i} - Y_{\text{predicted},i})^2, \quad (18)$$

$$R^2 = 1 - \frac{\sum_{i=1}^{N} (Y_{\text{observed},i} - Y_{\text{predicted},i})^2}{\sum_{i=1}^{N} (Y_{\text{observed},i} - Y_{\text{mean}})^2}, \quad (19)$$

where $Y_{\text{predicted},i}$ is the ith predicted value by the developed model, $Y_{\text{observed},i}$ is the ith observation, Y_{mean} is the average value of the observations and N is the number of data points.

Results and discussion

Statistical analysis of the dataset

A database encompassing the environmental conditions, FWD properties and placement configuration, fire behaviour and FWD combustion factor was established that included 17 independent variables. The statistical characteristics of key variables in the dataset are presented in Figs 3 and 4.

Fig. 3 shows the distribution of six variables encompassing environmental condition variables (i.e. ambient air temperature and RH) and pre-fire fuel property variables including both the FWD fuel load and pre-burn FWD diameter, as well as the direction of flame spread as a fire behaviour variable. Fig. 3*a*, *b* shows that ambient air temperature ranged from 22 to 31°C, while RH varied between 26.3 and 56.8%. These conditions reflect typical weather characteristics of March in Canberra, Australia. Fig. 3*c* shows that most of the data sets (110 entries) fell into the heading fire spread condition, with only 28 entries as backing fires. Fig. 3*d*, *e* shows the distribution of fuel load and pre-burn diameter of FWD. There are three FWD fuel load levels in the dataset, i.e. 0.2, 0.6, 1.2 kg m^{-2}, with the majority of observations corresponding to 0.6 kg m^{-2}. The pre-burn diameter is in accordance with a normal distribution, with most of the observations belonging to the 2.5–3 cm range.

Fig. 4 shows the distribution of fire behaviour variables as well as the FWD combustion factor as box plots, where the box chart on the left summarises key statistical measures, namely the maximum, upper bound, 75th percentile, median, mean, 25th percentile, lower bound and minimum values, and the right side shows each data point. The bounds (whiskers) of the box chart are determined using the 1.5 interquartile range method, and any data point less than the lower bound or more than the upper bound is classified as an outlier (Tukey 1977).

Downloaded from http://connectsci.au/wf/article-pdf/doi/10.1071/WF25255/1856354/wf25255.pdf by The Hong Kong Polytechnic University user on 13 February 2026

Fig. 4*a* illustrates the ignition delay and flame residence time for each FWD. The ignition delay ranges from 0 to 135 s, with a median of 5 s and a mean of 13 s. The flame residence time varies from 28.3 to 184.4 s, with a mean of 89.4 s. Notably, the majority of the ignition delay data points fall within the range of 0–20 s. Fig. 4*b* shows the duration of flaming and smouldering combustion for each piece of FWD. The flaming duration ranges from 2 to 28.5 min, following a normal distribution, with a median of 10.5 min. In contrast, the smouldering duration ranges from 0 to 30 min, with most data points concentrated within the 0–2.5 min range. The median smouldering duration is 1.5 min, while the mean is 5.2 min. The flame ROS and FLI are demonstrated in Fig. 4*c*, *d*. The interval and cumulative ROS are in the range of 4.2–93.5 and 4.8–61.1 m h^{-1}, respectively, with average values of 40.8 and 39.9 m h^{-1}. Moreover, the interval and cumulative FLI range from 17.4 to 649.4 and 20.5 to 429.2 kW m^{-1}, respectively, mainly corresponding to low-intensity fires, commensurate with the objective of achieving prescribed fire behaviour. Fig. 4*e* shows the box plot of charring intensity, indicating a median of 8.2 × 10^4 °C s and a mean of 1.1 × 10^5 °C s, with two identified outliers. Fig. 4*f* displays a box plot of the combustion factor for FWD, where the data points are clearly separated into two categories: 100% (fully consumed) and 0–60% (partially consumed). The mean value of the FWD combustion factor is 59.3%, while the median is 100%, meaning over 50% of FWD fuels were fully consumed by fire.

The Pearson correlation coefficient (r) is a common way of quantifying a linear correlation between two variables (Kader and Franklin 2008). Fig. 5 presents an r-matrix, where each row represents a variable in our dataset, and the columns represent the same variables as the rows. Within each cell, the colour (as explained by the colour bar) and the size of the square reflect the magnitude of the correlation coefficient (r-value) between the two variables. Additionally, the significance level of the correlation coefficient (P-value) is denoted by the number of asterisks in the cell. In general, larger squares with a darker colour indicate stronger linear correlations, and more asterisks signify higher statistical significance.

As shown in Fig. 5, a highly significant negative correlation ($P < 0.001$) is observed between the flame ROS (both interval and cumulative) and the ambient humidity ($r \approx -0.5$), direction of flame spread ($r \approx -0.9$) and tunnel position ($r \approx -0.5$). This indicates the flame ROS decreases with increasing environmental humidity and backing fires will lead to a smaller ROS (backing fires are labelled as 1 and heading fires are labelled as 0 in the dataset). A similar correlation pattern is also observed between the FLI and the ambient humidity, wind direction and tunnel position.

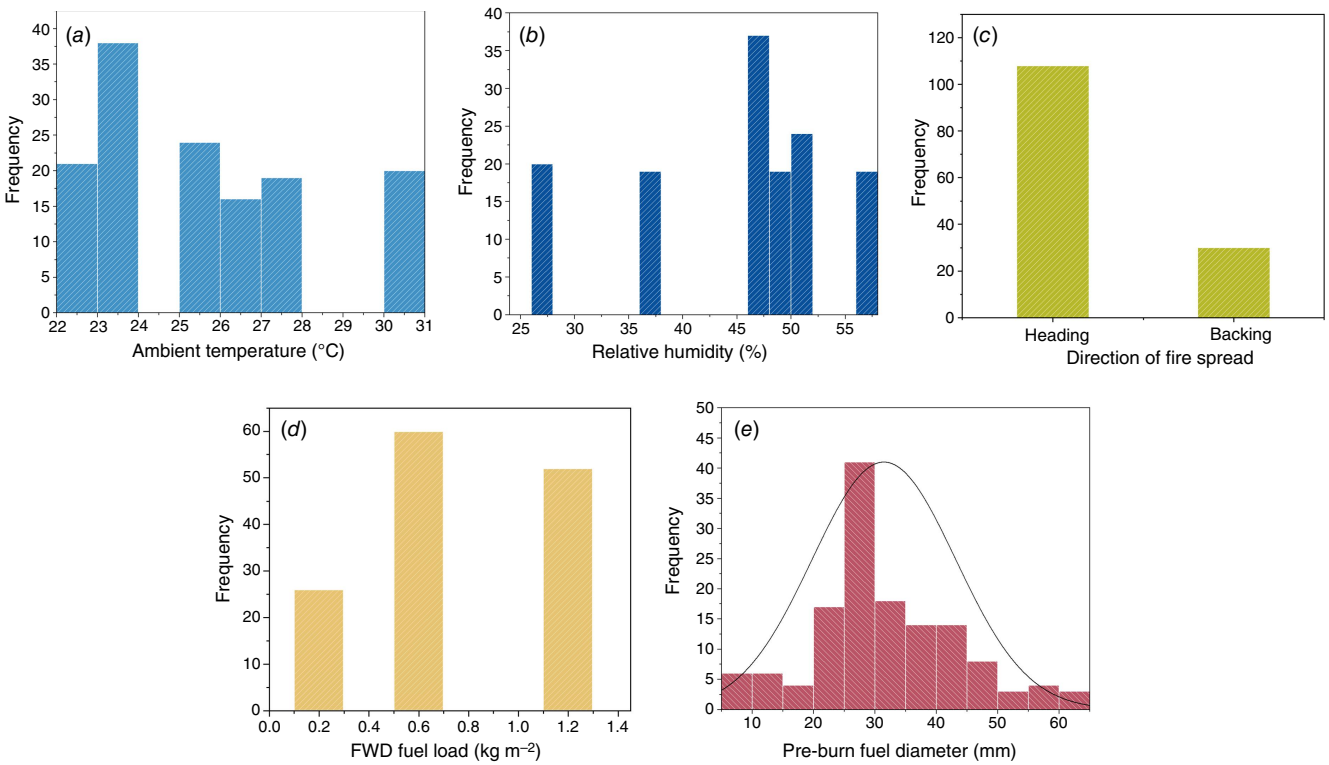

Fig. 3. Data distribution of the variables characterising the environmental conditions and pre-fire fuel properties in the dataset: (*a*) ambient temperature, (*b*) relative humidity, (*c*) direction of fire spread, (*d*) fuel load of FWD, and (*e*) pre-burn FWD diameter, where the curve in (*e*) indicates the fitted normal distribution.

Downloaded from http://connectsci.au/wf/article-pdf/doi/10.1071/WF25255/1856354/wf25255.pdf by The Hong Kong Polytechnic University user on 13 February 2026

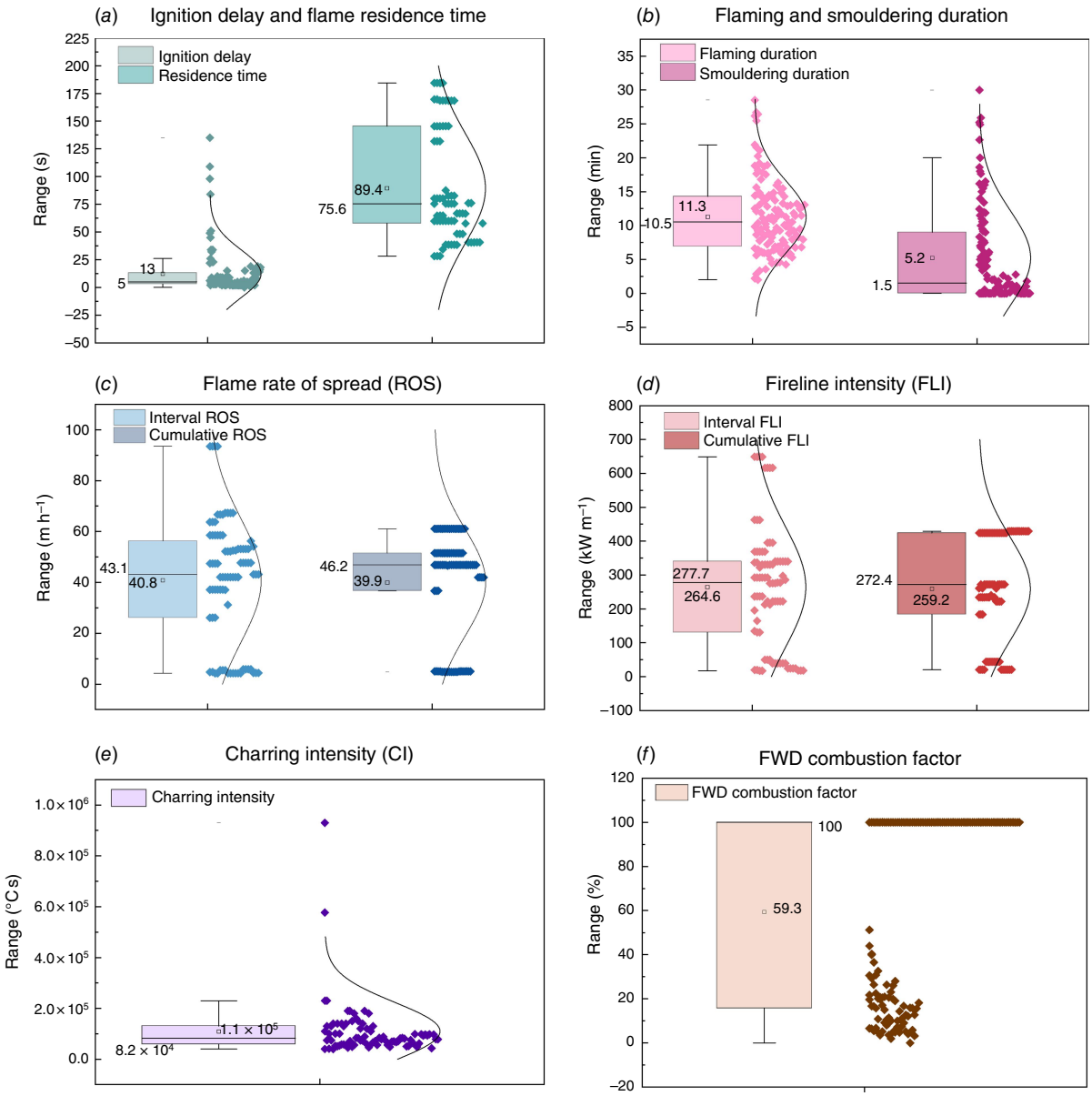

Fig. 4. Box plot with overlaid data distribution of the fire behaviour variables and FWD combustion factor in the dataset: (*a*) ignition delay and residence time, (*b*) duration of flaming and smouldering combustion, (*c*) interval and cumulative flame rate of spread, (*d*) interval and cumulative fireline intensity, (*e*) charring intensity, and (*f*) FWD combustion factor. In panels, the number next to the hollow square in the box plot represents the mean and the other quantity presented is the median.

Ignition delay shows a highly significant positive correlation with the direction of flame spread ($P < 0.001$, $r = 0.654$), suggesting the backing fire will increase the ignition delay of FWD. In addition, ignition delay is negatively correlated with both ROS and FLI, implying that a longer ignition delay always accompanies lower ROS and FLI. Flame residence time exhibits significant positive correlations with direction of flame spread ($r = 0.748$), fuel load ($r = 0.586$), tunnel position ($r = 0.399$) and pre-burn FWD diameter ($r = 0.396$), while showing strong negative correlations with ROS and FLI. Regarding the flaming duration, it is positively correlated with direction of flame spread and pre-burn diameter. However, smouldering duration only shows a highly significant correlation with pre-burn diameter ($P < 0.001$, $r = 0.454$). The CI shows a significant positive correlation with tunnel axial position ($P < 0.05$, $r = 0.285$). Overall, the analysis suggests that environmental humidity, direction of flame spread, FWD fuel load and tunnel axial position where FWD is placed are the four key variables that have a significant linear relationship with fire behaviour parameters. Both flaming and smouldering durations are more correlated with the pre-burn diameter.

Downloaded from http://connectsci.au/wf/article-pdf/doi/10.1071/WF25255/1856354/wf25255.pdf by The Hong Kong Polytechnic University user on 13 February 2026

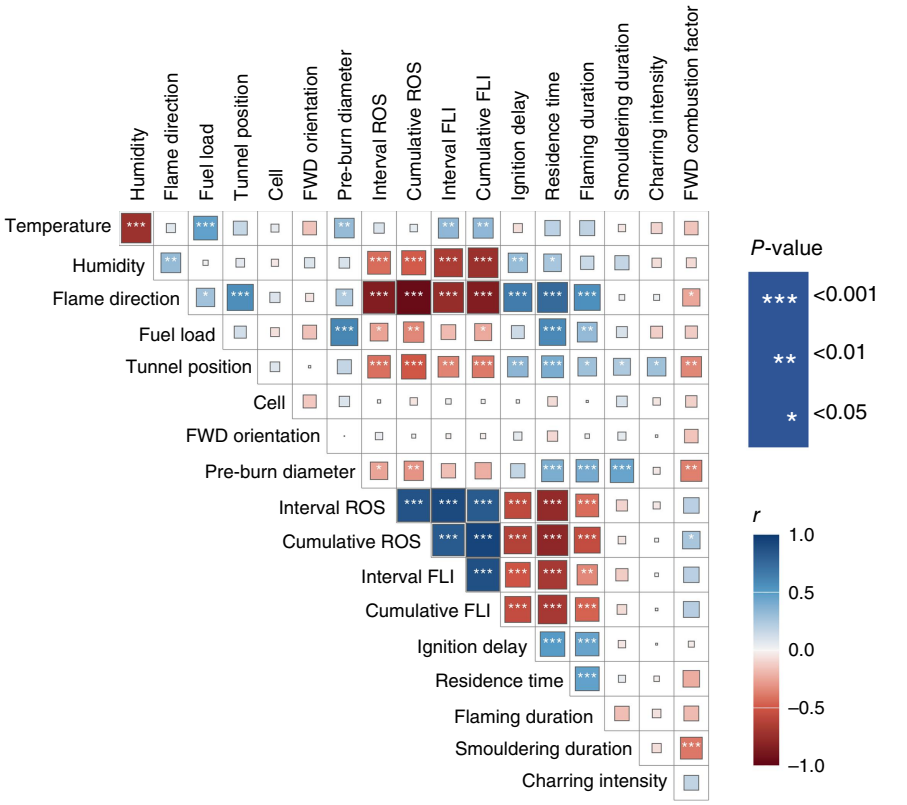

Fig. 5. Pearson correlation coefficient (r) among any two variables in the dataset with the P-value marked.

More importantly, it was identified that the combustion factor of FWD shows highly significant negative correlations with smouldering duration ($P < 0.001$), pre-burn diameter ($P < 0.01$) and tunnel axial position ($P < 0.01$).

Evaluation of the binary classification models

Five variables, namely direction of flame spread, fuel load of FWD, tunnel axial position where FWD is placed, orientation in which FWD is placed and FWD pre-burn diameter, were selected as the input features for the classification models. The models employed here include LR, RF, support vector classifiers with polynomial (SVC (P)) and RBF kernels and ANNs. The evaluation results, namely accuracy, precision, $F1$ score and AUC of the five-fold cross-validation of five different classification models, are shown in the box plot in Fig. 6. The degree of the SVC model polynomial kernel is 2 and the hidden layer size of the ANN model is (10.5). All other models are set as the default.

Fig. 6*a* shows that the SVC (P) model has a higher mean accuracy score than the other classifiers, with the mean being approximately 0.75. Fig. 6*b* shows that all the classification models have median precisions larger than 0.60 except for the RBF model. Fig. 6*c* shows the distribution of the $F1$ score, where both the median and average $F1$ score of the SVC (P) model are the highest, whereas RF model has the smallest $F1$ score. Fig. 6*d* shows the AUC under the ROC curve. It can be seen that the SVC models with a two-degree polynomial kernel achieve higher AUC values than others, with the median at ~0.78 and the average at 0.82. Overall, the SVC model with a two-degree polynomial kernel demonstrates better performance in classifying the fully consumed and partially consumed FWD, with median accuracy, $F1$ score and AUC of 0.74, 0.79 and 0.78, respectively.

Evaluation of the regression models

Prediction of fire behaviour variables

Three different ANN models, identified as ANN_1, ANN_2 and ANN_3, were developed to predict the fire behaviour variables including the flame ROS, the FLI, the flame residence time and the duration of flaming combustion. The hyper-parameters and the selected input features of the best training models were determined with five-fold cross-validation and were used to retrain the prediction model. The hyper-parameters and input features of each model, after optimisation by the trial-and-error method within the training set, are summarised in Table 1.

Eight variables, namely ambient air temperature, RH, flame spread direction, fuel load, tunnel axial position, cell position, FWD orientation and pre-burn diameter, are selected as input features for the ANN_1 and ANN_2 models to predict ROS and FLI. The models achieve cross-validation RMSE scores of 0.146 and 0.167, respectively. In comparison, six input variables are included in the ANN_3 model to

Downloaded from http://connectsci.au/wf/article-pdf/doi/10.1071/WF25255/1856354/wf25255.pdf by The Hong Kong Polytechnic University user on 13 February 2026

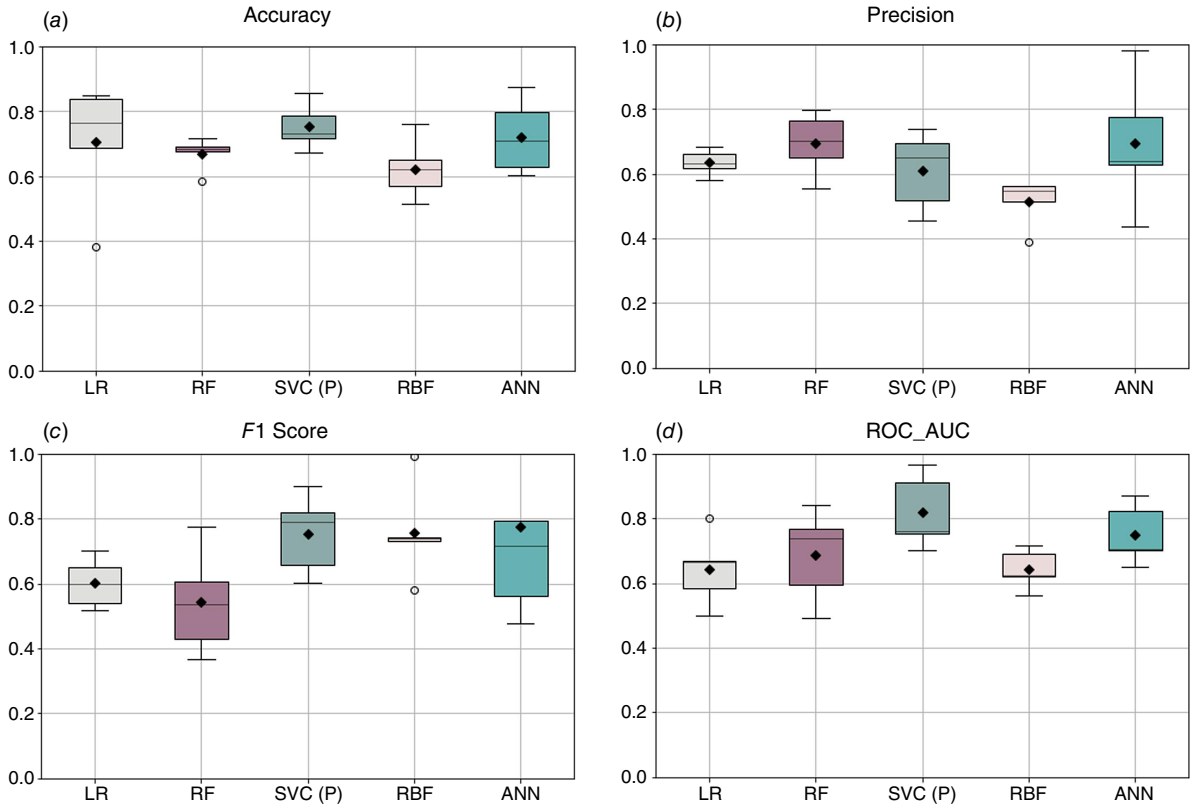

Fig. 6. Box-plot distributions of (*a*) accuracy, (*b*) precision, (*c*) *F*1 score, and (*d*) AUC under ROC curve of different classification models from the five-fold cross-validation, where the horziontal line in the box represents the median, the diamonds indicate the average values, the whiskers indicate ± 1.5 IQR, and circles represent outliers.

Table 1. Inputs, outputs and hyper-parameters of the developed ANN models.

	ANN_1	ANN_2	ANN_3
Output targets	Interval and cumulative ROS	Interval and cumulative FLI	Flame residence time and flaming duration
Input variables	Temperature, relative humidity, direction of flame spread, FWD fuel load, tunnel axial position, cell, FWD orientation, pre-burn diameter	Temperature, relative humidity, direction of flame spread, FWD fuel load, tunnel axial position, cell, FWD orientation, pre-burn diameter	Temperature, relative humidity, direction of flame spread, FWD fuel load, FWD orientation, pre-burn diameter
hidden_layer_size	8, 25, 8	8, 25, 8	8, 4
Activation function	relu	relu	relu
learning_rate_init	0.001	0.001	0.005
max_iter	10,000	10,000	10,000

predict the flame residence time and flaming duration, which achieves a cross-validation RMSE score of 0.177. Additionally, the loss functions of training and validation sets during the training process show that all the developed models reach convergence with a minimum MSE loss close to zero (see Supplementary Fig. S1*a–c*).

Fig. 7 shows the performance of each ANN model evaluated on the test datasets. Fig. 7*a*, *b* illustrates that, generally, the prediction results of ROS and FLI are good, with R^2 scores larger than 0.9. However, the accuracy of ANN_3 is less satisfactory, with R^2 of 0.69 for residence time and only 0.35 for flaming duration. The possible reasons for the poor performance include: (1) the dataset is small and contains only 71 data points with fire behaviour parameters, and (2) there is noise in the flame residence time and flaming duration, as they were manually extracted from video recordings. In addition, the position of the FWD pieces is not important in predicting the residence time and flaming duration; thus, only six input features are selected for model ANN_3.

Downloaded from http://connectsci.au/wf/article-pdf/doi/10.1071/WF25255/1856354/wf25255.pdf by The Hong Kong Polytechnic University user on 13 February 2026

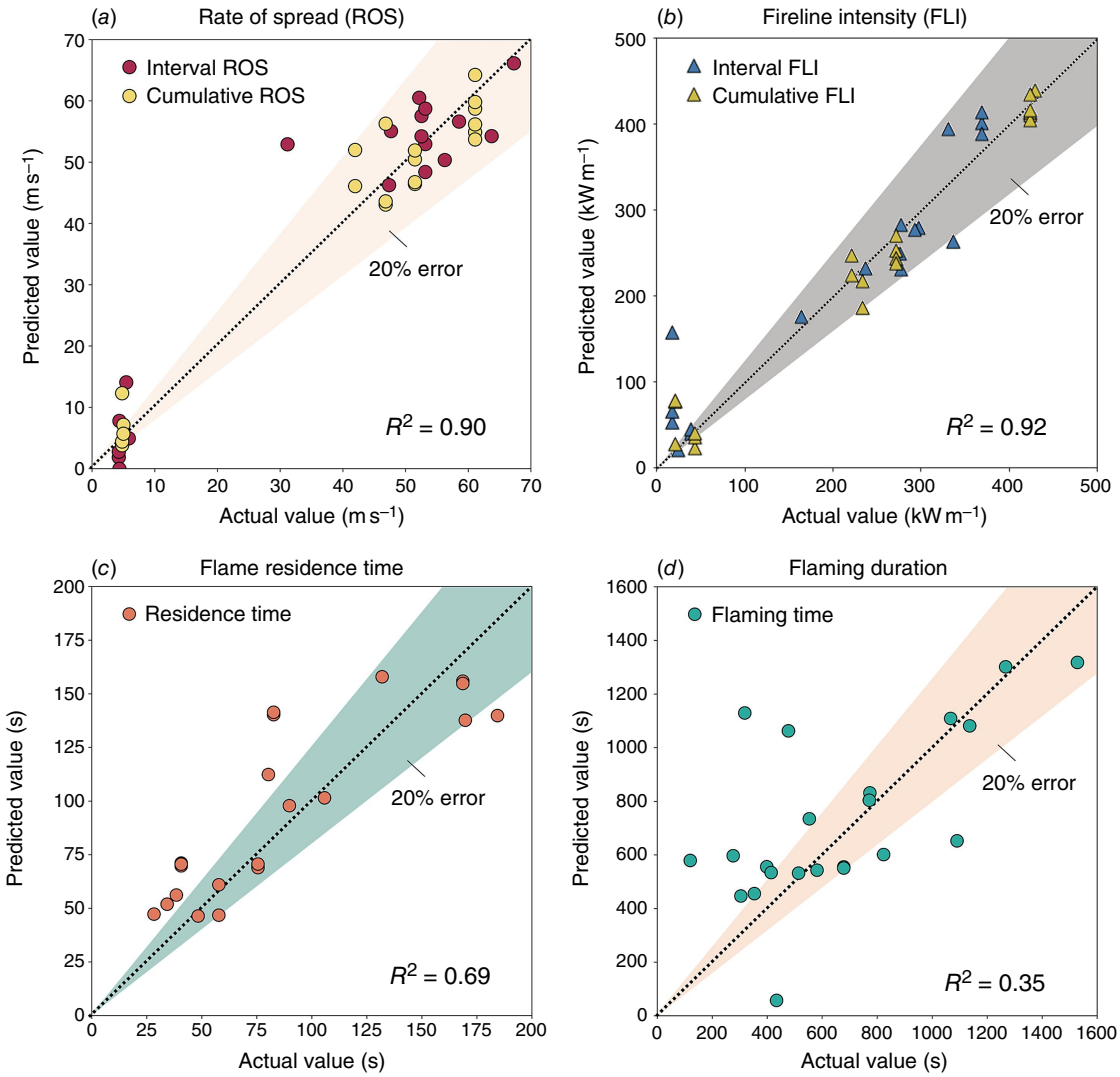

Fig. 7. Predicted versus observed values in the test datasets: (*a*) flame rate of spread, (*b*) fireline intensity, (*c*) flame residence time, and (*d*) flaming duration.

Table 2. Hyper-parameters and performance of different fuel consumption rate prediction models.

Models	RR	KNN	SVR	ANN
Hyper-parameters	alphas = np.logspace(-3, 3, 100)	*k* = 5	kernel = 'rbf', *C* = 1, epsilon = 1, gamma = 'scale'	hidden_layer_sizes = (32, 8), activation = 'relu', alpha = 0.01, learning_rate_init = 0.0001, tol = 0.00001
MAE (%)	8.65 ± 1.81	8.97 ± 2.50	8.72 ± 1.64	9.79 ± 2.26
RMSE (%)	9.98 ± 2.37	12.25 ± 1.50	10.20 ± 1.16	11.94 ± 1.10

Prediction of FWD combustion factors

Given that some fire behaviour parameters are missing in the dataset (present in only 71 out of 138 entries), the ANN models developed in the former sub-section are employed to predict the missing values, thus creating a more complete dataset. In total, the dataset of incompletely combusted FWD pieces includes 67 data points. Four regression models, RR, KNN, SVR and ANN, were selected to predict the combustion factor of the partially consumed FWD.

Table 2 summarises the best hyper-parameters and the performance of each model trained with five-fold cross-validation. As illustrated, the predictive performance of all models is fairly poor in terms of the MAE and RMSE values. Specifically, the MAE is approximately 9%, while the RMSE is ~11%. Among all models, RR demonstrates the best performance, achieving an average MAE of 8.7% and RMSE of 10.0%. The poor performance of the prediction models for the combustion factor of partially consumed

Downloaded from http://connectsci.au/wf/article-pdf/doi/10.1071/WF25255/1856354/wf25255.pdf by The Hong Kong Polytechnic University user on 13 February 2026

FWD can be attributed to the following reasons: (1) the dataset is small (with only 67 available entries), limiting the models' ability to generalise and detect complex non-linear patterns; (2) there is noise in the dataset, as measurement and data collection errors are inevitable during manual processing from a single overhead camera; and (3) the correlation between the input features and the FWD combustion factor is weak (as indicated by the *P*-value matrix in Fig. 5). Future work should prioritise data enrichment, both in terms of increasing the number of samples and incorporating more relevant features.

Implications for woody fuel consumption modelling

Collection of quality-controlled data on woody fuel consumption is a key priority for wildland fire management as well as global carbon accounting. This is owing to the significant contribution that WD consumption in wildland fires (wild and prescribed) makes to greenhouse gas emissions and the large uncertainties that exist in woody fuel combustion factors (French *et al.* 2004; Surawski *et al.* 2016), as well as the globally limited nature of woody fuel field measurement databases (Van Leeuwen *et al.* 2014). In the present study, we explored FWD consumption dynamics in a combustion wind tunnel facility that allowed collection of high-quality data under controlled conditions that are difficult to obtain in the field. This outcome was achieved through tight control of experimental variables that are known to influence FWD consumption, such as fuel load, fuel architecture and wind speed.

The Pearson correlation matrix presented in Fig. 5 shows that five explanatory variables are correlated with FWD consumption in a statistically significant manner. At a 5% level of significance, cumulative surface fire ROS is positively correlated with FWD consumption and heading fires were identified to consume more FWD than backing fires. Both of these findings concur with previous research results suggesting the FLI is a key predictor of FWD consumption (Hollis *et al.* 2011*a*). At a 1% level of significance, FWD consumption is negatively correlated with pre-burn diameter and tunnel axial position, whereas at a 0.1% level of significance, FWD is negatively correlated with smouldering duration. The relationship between FWD consumption and pre-burn diameter is consistent with previous studies suggesting that smaller-diameter FWD fuels receive greater rates of heat transfer from a surface fire than larger-diameter fuels and, as a result, FWD consumption is increased owing to its greater surface area-to-volume ratio (Ottmar 2014). The relationship between FWD consumption and tunnel axial position stems from previous work by Sullivan *et al.* showing that cumulative ROS in the CSIRO Pyrotron gradually increases to a pseudo-steady state after 4 m of forward spread in the presence of FWD (Sullivan *et al.* 2018). This finding adds further evidence to the claim that FLI is driving FWD consumption. The strong negative correlation between smouldering duration and FWD consumption suggests that complete burnout of FWD (with limited smouldering durations) is achieved quickly in some fires (especially heading fires), whereas incomplete burnout of FWD occurs in some fires (especially backing fires) with longer smouldering durations. This finding suggests that backing fires generally did not carry sufficient heat flux to completely burn out FWD pieces based on the environmental conditions experienced during our fires. Another key finding from our study is that combustion wind tunnel experiments capture the basic fire behaviour physics that is required to understand FWD consumption.

Our study offers new insights into the prediction of FWD consumption by leveraging ML techniques. The proposed hybrid framework firstly classifies FWD as fully consumed and partially consumed, and then creates regression models to estimate the combustion factor for partially consumed FWD pieces. Our framework achieves promising results, with classification accuracy of 74% using the SVC model and an MAE of 8.7% in the regression task using a RR model. Compared with the GLM employed by Hollis *et al.* (2011*b*), which reported an MAE of 10%, our models achieved a slightly higher predictive accuracy. We largely attribute this result to improvement in the availability of statistical models, including ML that can more easily handle complex and non-linear interactions among input variables. Continued exploration of ML techniques in FWD modelling will further improve predictions given the non-linear behaviour of woody fuel consumption.

Conclusions

Data collected during experiments conducted previously in the CSIRO Pyrotron combustion wind tunnel were analysed to investigate the consumption of fine woody debris (FWD) with diameters ranging from 6 to 50 mm. Eighteen variables from the laboratory fires were measured and collected to form a database. These included measures of environmental conditions (ambient air temperature, relative humidity and wind speed), FWD properties (fuel load, pre- and post-fire diameters), FWD arrangement (tunnel axial position, cell position, orientation) and fire behaviour (rate of spread, fireline intensity, ignition delay, flame residence time, flaming duration, smouldering duration and charring intensity). Pearson correlation coefficient analysis revealed that the combustion factor of FWD pieces exhibited highly significant negative correlations with their smouldering duration ($P < 0.001$), pre-burn diameter ($P < 0.01$) and tunnel axial position ($P < 0.01$).

Based on the database, binary classification models were first developed to classify the FWD pieces as fully consumed (combustion factor = 100%) or partially consumed ($0 \leq$ combustion factor $< 100\%$), followed by regression models

Downloaded from http://connectsci.au/wf/article-pdf/doi/10.1071/WF25255/1856354/wf25255.pdf by The Hong Kong Polytechnic University user on 13 February 2026

to predict the specific combustion factor among the partially consumed FWD. The results show that the support vector classifier (SVC) with a two-degree polynomial kernel outperformed other classifiers, achieving an accuracy of 0.74 and an AUC score of 0.78. The performance of the regression models for predicting the combustion factor of partially consumed FWD had an average MAE of ~9% and an RMSE of ~11%. In addition, the developed ANN models can successfully predict the fire rate of spread and fireline intensity, with R^2 scores larger than 0.9. Future work should prioritise data enrichment, both in terms of increasing the number of samples (up to ~300) and incorporating more relevant features such as moisture content and decay status, to improve the machine learning model performance. Furthermore, it would be valuable to test and evaluate the models against truly independent field data to assess their real-world applicability and robustness.

Nomenclature

Symbols

ANN	Artificial neural network
AUC	Area under curve
CI	Charring intensity (°C s)
d (or D)	Diameter (cm)
FL	Fuel load (kg m^{-2})
FLI	Fireline intensity (kW m^{-1})
FN	False negatives
FP	False positives
FPR	False Positive Rate
FWD	Fine woody debris
GLM	Generalised linear model
H	Lower heat of combustion (kJ kg^{-1})
KNN	K-nearest neighbours
LR	Logistic regression
MAE	Mean absolute error
MC	Moisture content (%)
ML	Machine learning
MLR	Multiple Linear Regression
PAR	Parallel
PER	Perpendicular
RBF	Radial Basis Function
RF	Random forest
RH	Relative humidity (%)
RMSE	Root mean squared error
ROS	Rate of spread (m s^{-1})
ROC	Receiver operating characteristic
WFCP	Woody Fuel Consumption Project
RR	Ridge regression
SVC	Support Vector Classifier
SVM	Support vector machine
SVR	Support vector regression
t	Time (s or min)
T	Temperature (°C)
TN	True negatives
TP	True positives
TPR	True Positive Rate
w	mass of fuel consumed in the flaming front per unit area (kg m^{-2})
WD	Woody debris
WFCP	Woody Fuel Consumption Project

Subscripts

a	ambient
cu	cumulative
fl	flaming combustion
pre	pre-burn
ig	ignition
in	interval
re	residence of flame
sm	smouldering combustion

Supplementary material

Supplementary material is available online.

References

Albini FA (1976) 'Computer-based models of wildland fire behavior: a user's manual.' (Forest Service, Intermountain Forest and Range Experiment Station: USA)

Albini FA, Reinhardt ED (1995) Modeling ignition and burning rate of large woody natural fuels. *International Journal of Wildland Fire* **5**, 81–91. doi:10.1071/WF9950081

Albini FA, Reinhardt ED (1997) Improved calibration of a large fuel burnout model. *International Journal of Wildland Fire* **7**, 21–28. doi:10.1071/WF9970021

Altman NS (1992) An introduction to kernel and nearest-neighbor nonparametric regression. *American Statistician* **46**, 175–185. doi:10.1080/00031305.1992.10475879

Bassett M, Chia EK, Leonard SWJ, Nimmo DG, Holland GJ, Ritchie EG, Clarke MF, Bennett AF (2015) The effects of topographic variation and the fire regime on coarse woody debris: insights from a large wildfire. *Forest Ecology and Management* **340**, 126–134. doi:10.1016/j.foreco.2014.12.028

Bennett ND, Croke BFW, Guariso G, Guillaume JHA, Hamilton SH, Jakeman AJ, Marsili-Libelli S, Newham LTH, Norton JP, Perrin C, Pierce SA, Robson B, Seppelt R, Voinov AA, Fath BD, Andreassian V (2013) Characterising performance of environmental models. *Environmental Modelling and Software* **40**, 1–20. doi:10.1016/j.envsoft.2012.09.011

Bisong E (2019) Introduction to Scikit-learn. In 'Building Machine Learning and Deep Learning Models on Google Cloud Platform: A Comprehensive Guide for Beginners'. pp. 215–229. (Springer)

Breiman L (2001) Random forests. *Machine Learning* **45**, 5–32. doi:10.1023/A:1010933404324

Brown JK (1985) 'Predicting duff and woody fuel consumed by prescribed fire in the northern Rocky Mountains.' (USDA Forest Service, Intermountain Forest and Range)

Burrows ND (2001) Flame residence times and rates of weight loss of eucalypt forest fuel particles. *International Journal of Wildland Fire* **10**, 137–143. doi:10.1071/WF01005

Byram GM (1959) Combustion of forest fuels. In 'Forest Fire: Control and Use' (Ed. KP Davis) pp. 61–89. (McGraw-Hill)

Chen Y, Wang Z, Lin S, Qin Y, Huang X (2023) A review on biomass thermal-oxidative decomposition data and machine learning prediction of thermal analysis. *Cleaner Materials* **9**, 100206. doi:10.1016/j.clema.2023.100206

Chetehouna K, El Tabach E, Bouazaoui L, Gascoin N (2015) Predicting the flame characteristics and rate of spread in fires propagating in a bed of *Pinus pinaster* using Artificial Neural Networks. *Process Safety and Environmental Protection* **98**, 50–56. doi:10.1016/j.psep.2015.06.010

Cortes C, Vapnik V (1995) Support-Vector Networks. *Machine Learning* **20**(3), 273–297. doi:10.1007/BF00994018

Downloaded from http://connectsci.au/wf/article-pdf/doi/10.1071/WF25255/1856354/wf25255.pdf by The Hong Kong Polytechnic University user on 13 February 2026

Davis MR, Allen RB, Clinton PW (2003) Carbon storage along a stand development sequence in a New Zealand Nothofagus forest. *Forest Ecology and Management* **177**, 313–321. doi:10.1016/S0378-1127(02)00333-X

De Groot WJ, Pritchard JM, Lynham TJ (2009) Forest floor fuel consumption and carbon emissions in Canadian boreal forest fires. *Canadian Journal of Forest Research* **39**, 367–382. doi:10.1139/X08-192

Duane A, Pique M, Castellnou M, Brotons L (2015) Predictive modelling of fire occurrences from different fire spread patterns in Mediterranean landscapes. *International Journal of Wildland Fire* **24**, 407–418. doi:10.1071/WF14040

Finney MA, McAllister SS (2011) A review of fire interactions and mass fires. *Journal of Combustion* **2011**, 548328. doi:10.1155/2011/548328

French NHF, Goovaerts P, Kasischke ES (2004) Uncertainty in estimating carbon emissions from boreal forest fires. *Journal of Geophysical Research Atmospheres* **109**, 1–12. doi:10.1029/2003JD003635

Gould JS, Sullivan AL (2021) Initial growth of fires in eucalypt litter, from ignition to steady-state rate of spread: laboratory studies. *International Journal of Wildland Fire* **31**, 163–175. doi:10.1071/WF21094

Gould JS, Sullivan AL, Hurley R, Koul V (2017) Comparison of three methods to quantify the fire spread rate in laboratory experiments. *International Journal of Wildland Fire* **26**, 877–883. doi:10.1071/WF17038

Guérette ÉA, Paton-Walsh C, Desservettaz M, Reisen F, Surawski NC, Meyer CPM, Roulston CT, Sullivan A, Weston CJ, Volkova L (2025) Simplifying emissions modelling from wildland fires: laboratory-scale emission factors are independent of fine woody debris fuel load. *International Journal of Wildland Fire* **34**, WF24117. doi:10.1071/WF24117

Harmon ME, Franklin JF, Swanson FJ, Sollins P, Gregory SV, Lattin JD, Anderson NH, Cline SP, Aumen NG, Sedell JR (1986) Ecology of coarse woody debris in temperate ecosystems. *Advances in Ecological Research* **15**, 133–302. doi:10.1016/S0065-2504(08)60121-X

Hodges JL, Lattimer BY (2019) Wildland fire spread modeling using convolutional neural networks. *Fire Technology* **55**, 2115–2142. doi:10.1007/s10694-019-00846-4

Hollis JJ, Matthews S, Ottmar RD, Prichard SJ, Slijepcevic A, Burrows ND, Ward B, Tolhurst KG, Anderson WR, Gould JS (2010) Testing woody fuel consumption models for application in Australian southern eucalypt forest fires. *Forest Ecology and Management* **260**, 948–964. doi:10.1016/j.foreco.2010.06.007

Hollis JJ, Anderson WR, McCaw WL, Cruz MG, Burrows ND, Ward B, Tolhurst KG, Gould JS (2011*a*) The effect of fireline intensity on woody fuel consumption in southern Australian eucalypt forest fires. *Australian Forestry* **74**, 81–96. doi:10.1080/00049158.2011.10676350

Hollis JJ, Matthews S, Anderson WR, Cruz MG, Burrows ND (2011*b*) Behind the flaming zone: predicting woody fuel consumption in eucalypt forest fires in southern Australia. *Forest Ecology and Management* **261**, 2049–2067. doi:10.1016/j.foreco.2011.02.031

Hollis AA, McCaw WL, Cruz MG (2018) The effect of woody fuel characteristics on fuel ignition and consumption: a case study from a eucalypt forest in south-west Western Australia. *International Journal of Wildland Fire* **27**, 363–375. doi:10.1071/WF17174

Hong H, Tsangaratos P, Ilia I, Liu J, Zhu A-X, Xu C (2018) Applying genetic algorithms to set the optimal combination of forest fire related variables and model forest fire susceptibility based on data mining models. The case of Dayu County, China. *Science of The Total Environment* **630**, 1044–1056. doi:10.1016/j.scitotenv.2018.02.278

Hough WA (1968) 'Fuel consumption and fire behavior of hazard reduction burns.' (USDA Forest Service, Southeastern Forest Experiment)

Hyde JC, Smith AMS, Ottmar RD, Alvarado EC, Morgan P (2011) The combustion of sound and rotten coarse woody debris: a review. *International Journal of Wildland Fire* **20**, 163–174. doi:10.1071/WF09113

Jafari Goldarag Y, Mohammadzadeh A, Ardakani AS (2016) Fire risk assessment using neural network and logistic regression. *Journal of the Indian Society of Remote Sensing* **44**, 885–894. doi:10.1007/s12524-016-0557-6

Jain P, Coogan SCP, Subramanian SG, Crowley M, Taylor S, Flannigan MD (2020) A review of machine learning applications in wildfire science and management. *Environmental Reviews* **28**, 478–505. doi:10.1139/er-2020-0019

James G, Witten D, Hastie T, Tibshirani R (2013) 'An introduction to statistical learning.' (Springer)

Kader G, Franklin C (2008) The evolution of Pearson's correlation coefficient. *Mathematics Teacher* **102**, 292–299. doi:10.5951/MT.102.4.0292

Kartal F, Özveren U (2022) Investigation of the chemical exergy of torrefied biomass from raw biomass by means of machine learning. *Biomass and Bioenergy* **159**, 106383. doi:10.1016/j.biombioe.2022.106383

Kauffman JB, Martin RE (1989) Fire behavior, fuel consumption, and forest-floor changes following prescribed understory fires in Sierra Nevada mixed conifer forests. *Canadian Journal of Forest Research* **19**, 455–462. doi:10.1139/x89-071

Knapp EE, Keeley JE, Ballenger EA, Brennan TJ (2005) Fuel reduction and coarse woody debris dynamics with early season and late season prescribed fire in a Sierra Nevada mixed conifer forest. *Forest Ecology and Management* **208**, 383–397. doi:10.1016/j.foreco.2005.01.016

Kozik VI, Nezhevenko ES, Feoktistov AS (2013) Adaptive prediction of forest fire behavior on the basis of recurrent neural networks. *Optoelectronics, Instrumentation and Data Processing* **49**, 250–259. doi:10.3103/S8756699013030060

LaValley MP (2008) Logistic regression. *Circulation* **117**, 2395–2399. doi:10.1161/CIRCULATIONAHA.106.682658

Liaw A, Wiener M (2002) Classification and Regression by randomForest. *R News* **2**, 18–22.

López-Serrano PM, López-Sánchez CA, Álvarez-González JG, García-Gutiérrez J (2016) A comparison of machine learning techniques applied to Landsat-5 TM spectral data for biomass estimation. *Canadian Journal of Remote Sensing* **42**, 690–705. doi:10.1080/07038992.2016.1217485

Manies KL, Harden JW, Bond-Lamberty BP, O'neill KP (2005) Woody debris along an upland chronosequence in boreal Manitoba and its impact on long-term carbon storage. *Canadian Journal of Forest Research* **35**, 472–482. doi:10.1139/x04-179

Montgomery DC, Runger GC (2010) 'Applied statistics and probability for engineers.' (John Wiley & Sons)

Mulvaney JJ, Sullivan AL, Cary GJ, Bishop GR (2016) Repeatability of free-burning fire experiments using heterogeneous forest fuel beds in a combustion wind tunnel. *International Journal of Wildland Fire* **25**, 445–455. doi:10.1071/WF15068

Nelson RM Jr (2003) Reaction times and burning rates for wind tunnel headfires. *International Journal of Wildland Fire* **12**, 195–211. doi:10.1071/WF02041

Ottmar RD (2014) Wildland fire emissions, carbon, and climate: modeling fuel consumption. *Forest Ecology and Management* **317**, 41–50. doi:10.1016/j.foreco.2013.06.010

Ottmar RD, Prichard SJ, Vihnanek RE, Sandberg DV (2006) 'Modification and validation of fuel consumption models for shrub and forested lands in the Southwest, Pacific Northwest, Rockies, Midwest, Southeast, and Alaska.' Final Project Report. pp. 91–98. (US Bureau of Land Management, Joint Fire Sciences Program)

Ottmar RD, Miranda AI, Sandberg DV (2008) Characterizing sources of emissions from wildland fires. *Developments in Environmental Science* **8**, 61–78. doi:10.1016/S1474-8177(08)00003-X

Pierce AD, Farris CA, Taylor AH (2012) Use of random forests for modeling and mapping forest canopy fuels for fire behavior analysis in Lassen Volcanic National Park, California, USA. *Forest Ecology and Management* **279**, 77–89. doi:10.1016/j.foreco.2012.05.010

Plucinski MP, Sullivan AL, Hurley RJ (2017) A methodology for comparing the relative effectiveness of suppressant enhancers designed for the direct attack of wildfires. *Fire Safety Journal* **87**, 71–79. doi:10.1016/j.firesaf.2016.12.005

Prichard SJ, Ottmar, RD Anderson GK (2006) 'Consume 3.0 user's guide. Pacific Wildland Fire Sciences Laboratory'. pp. 1–234 (USDA Forest Service, Seattle, WA)

Prichard SJ, Kennedy MC, Wright CS, Cronan JB, Ottmar RD (2017) Predicting forest floor and woody fuel consumption from prescribed burns in southern and western pine ecosystems of the United States. *Forest Ecology and Management* **405**, 328–338. doi:10.1016/j.foreco.2017.09.025

Pyle LA, Hockaday WC, Boutton T, Zygourakis K, Kinney TJ, Masiello CA (2015) Chemical and isotopic thresholds in charring: implications for the interpretation of charcoal mass and isotopic data. *Environmental Science and Technology* **49**, 14057–14064. doi:10.1021/acs.est.5b03087

Downloaded from http://connectsci.au/wf/article-pdf/doi/10.1071/WF25255/1856354/wf25255.pdf by The Hong Kong Polytechnic University user on 13 February 2026

Reinhardt ED (2003) Using FOFEM 5.0 to estimate tree mortality, fuel consumption, smoke production and soil heating from wildland fire. In 'Proceedings of the 2nd International Wildland Fire Ecology and Fire Management Congress and 5th Symposium on Fire and Forest Meteorology'. 16–20 November 2003. (American Meteorological Society: Boston, MA, USA)

Reinhardt ED, Keane RE, Brown JK (1997) 'First order fire effects model: FOFEM 4.0, users guide. Forest Service general technical report.' (Forest Service, Intermountain Research Station: Ogden, UT, USA)

Reinhardt ED, Keane RE, Brown JK (2001) Modeling fire effects. *International Journal of Wildland Fire* **10**, 373–380. doi:10.1071/WF01035

Riley KL, Grenfell IC, Finney MA, Crookston NL (2014) Utilizing random forests imputation of forest plot data for landscape-level wildfire analyses. In 'Advances in Forest Fire Research. Coimbra'. (Eds Viegas, D Xavier) pp. 583–590. (Imprensa da Universidade de Coimbra: Portugal) doi:10.14195/978-989-26-0884-6_67

Sullivan AL (2017) Inside the inferno: fundamental processes of wildland fire behaviour: Part 2: Heat transfer and interactions. *Current Forestry Reports* **3**, 150–171. doi:10.1007/s40725-017-0058-z

Sullivan AL, Ball R (2012) Thermal decomposition and combustion chemistry of cellulosic biomass. *Atmospheric Environment* **47**, 133–141. doi:10.1016/j.atmosenv.2011.11.022

Sullivan AL, McCaw WL, Cruz MG, Matthews S, Ellis PF (2012) Fuel, fire weather and fire behaviour in Australian ecosystems. In 'Flammable Australia fire regimes, Biodiversity Ecosystems a Changing world' (Eds RA Bradstock, AM Gill, RD Williams) pp. 51–77.

Sullivan AL, Surawski NC, Crawford D, Hurley RJ, Volkova L, Weston CJ, Meyer CP (2018) Effect of woody debris on the rate of spread of surface fires in forest fuels in a combustion wind tunnel. *Forest Ecology and Management* **424**, 236–245. doi:10.1016/j.foreco.2018.04.039

Surawski NC, Sullivan AL, Meyer CP, Roxburgh SH, Polglase PJ (2015) Greenhouse gas emissions from laboratory-scale fires in wildland fuels depend on fire spread mode and phase of combustion. *Atmospheric Chemistry and Physics* **15**, 5259–5273. doi:10.5194/acp-15-5259-2015

Surawski NC, Sullivan AL, Roxburgh SH, Polglase PJ (2016) Estimates of greenhouse gas and black carbon emissions from a major Australian wildfire with high spatiotemporal resolution. *Journal of Geophysical Research* **121**, 9892–9907. doi:10.1002/2016JD025087

Surawski NC, Macdonald LM, Baldock JA, Sullivan AL, Roxburgh SH, Polglase PJ (2020) Exploring how fire spread mode shapes the composition of pyrogenic carbon from burning forest litter fuels in a combustion wind tunnel. *Science of The Total Environment* **698**, 134306. doi:10.1016/j.scitotenv.2019.134306

Tang X, Machimura T, Li J, Yu H, Liu W (2022) Evaluating seasonal wildfire susceptibility and wildfire threats to local ecosystems in the largest forested area of China. *Earth's Future* **10**, e2021EF002199. doi:10.1029/2021EF002199

Tolhurst KG, Anderson WR, Gould J (2006) Woody fuel consumption experiments in an undisturbed forest. *Forest Ecology and Management* **234**, S109–S109. doi:10.1016/j.foreco.2006.08.145

Tukey JW (1977) 'Exploratory data analysis.' (Springer)

Van Leeuwen TT, Van Der Werf GR, Hoffmann AA, Detmers RG, Rücker G, French NHF, Archibald S, Carvalho JA, Cook GD, De Groot WJ, Hély C, Kasischke ES, Kloster S, McCarty JL, Pettinari ML, Savadogo P, Alvarado EC, Boschetti L, Manuri S, Meyer CP, Siegert F, Trollope LA, Trollope WSW (2014) Biomass burning fuel consumption rates: a field measurement database. *Biogeosciences* **11**, 7305–7329. doi:10.5194/bg-11-7305-2014

Vasilakos C, Kalabokidis K, Hatzopoulos J, Matsinos I (2009) Identifying wildland fire ignition factors through sensitivity analysis of a neural network. *Natural Hazards* **50**, 125–143. doi:10.1007/s11069-008-9326-3

Volkova L, Weston CJ (2015) Carbon loss from planned fires in southeastern Australian dry *Eucalyptus* forests. *Forest Ecology and Management* **336**, 91–98. doi:10.1016/j.foreco.2014.10.018

Volkova L, Roxburgh SH, Surawski NC, Meyer CP(Mick, Weston CJ (2019) Improving reporting of national greenhouse gas emissions from forest fires for emission reduction benefits: an example from Australia. *Environmental Science & Policy* **94**, 49–62. doi:10.1016/j.envsci.2018.12.023

Volkova L, Paul KI, Roxburgh SH, Weston CJ (2022) Tree mortality and carbon emission as a function of wildfire severity in south-eastern Australian temperate forests. *Science of The Total Environment* **853**, 158705. doi:10.1016/j.scitotenv.2022.158705

Youngblood A, Wright CS, Ottmar RD, McIver JD (2008) Changes in fuelbed characteristics and resulting fire potentials after fuel reduction treatments in dry forests of the Blue Mountains, northeastern Oregon. *Forest Ecology and Management* **255**, 3151–3169. doi:10.1016/j.foreco.2007.09.032

Zhang G, Wang M, Liu K (2021) Deep neural networks for global wildfire susceptibility modelling. *Ecological Indicators* **127**, 107735. doi:10.1016/j.ecolind.2021.107735

Data availability. Processed data from our experiment are available in Supplementary Table S1. Raw data will be made available on request.

Conflicts of interest. Andrew L. Sullivan and Xinyan Huang are Associate Editors of *International Journal of Wildland Fire* but were not involved in the peer review or decision-making process for this paper. The authors have no further conflicts of interest to declare.

Declaration of funding. We acknowledge funding from the Victorian Department of Environment, Land, Water and Planning. XH is supported by the National Natural Science Foundation of China (NSFC No. 52322610) and Hong Kong Research Grants Council GRF Scheme (No. 15221523).

Acknowledgements. The authors thank Martin Cope of CSIRO Oceans and Atmosphere for leading the overall project and Mick Meyer, Fabienne Reisen, Camila Trindade, Grant Edwards (deceased), Dean Howard, Stephen Wilson, Clare Murphy (née Paton-Walsh), Elise-Andrée Guérette, Maximilien Desservettaz and Valentina Wheeler for their assistance during the experimental programme. ALS thanks Debbie Crawford for her efforts in preliminary analysis and data reduction of the fire spread videos. NCS thanks Michael Battaglia and Sandra Eady for their support of this project.

Author contributions. Yuying Chen: conceptualisation, investigation, writing – original draft, formal analysis. Andrew L. Sullivan: conceptualisation, methodology, supervision, formal analysis, investigation, resources, data curation, project administration, funding acquisition, writing – review and editing. Zilong Wang: methodology, formal analysis. Liubov Volkova: methodology, investigation, resources, writing – review and editing, supervision. Christopher J. Weston: methodology, investigation, resources, writing – review and editing, supervision. Shaorun Lin: formal analysis. Yunzhu Qin: formal analysis. Xinyan Huang: supervision, writing – review and editing, funding acquisition. Nic C. Surawski: conceptualisation, methodology, formal analysis, investigation, resources, data curation, writing – review and editing, supervision.

Author affiliations

[A]Centre for Green Technology, University of Technology Sydney, Gadigal Country, PO Box 123, Ultimo, NSW 2007, Australia.

[B]State Key Laboratory of Climate Resilience for Coastal Cities, The Hong Kong Polytechnic University, Hong Kong.

[C]CSIRO Environment, GPO Box 1700, Canberra, ACT 2601, Australia.

[D]School of Agriculture, Food and Ecosystem Sciences, University of Melbourne, Creswick, VIC 3363, Australia.

Downloaded from http://connectsci.au/wf/article-pdf/doi/10.1071/WF25255/1856354/wf25255.pdf by The Hong Kong Polytechnic University user on 13 February 2026